Poly(propylene carbonate): Insight Into the Microstructure and Enantioselective Ring Opening Mechanism

ARTICLE *in* MACROMOLECULES · AUGUST 2012

Impact Factor: 5.8 · DOI: 10.1021/ma301916r

4 AUTHORS, INCLUDING:

Khalifah Salmeia
University of Jordan
3 PUBLICATIONS **17** CITATIONS

SEE PROFILE

Macromolecules

Article

pubs.acs.org/Macromolecules

Poly(propylene carbonate): Insight into the Microstructure and Enantioselective Ring-Opening Mechanism

Khalifah A. Salmeia, Sergei Vagin, Carly E. Anderson, and Bernhard Rieger*

WACKER-Lehrstuhl für Makromolekulare Chemie, Technische Universität München, Lichtenbergstrasse 4, 85747 Garching bei München, Germany

Supporting Information

ABSTRACT: Different poly(propylene carbonate) (PPC) microstructures have been synthesized from the alternating copolymerization of CO_2 with both racemic propylene oxide (PO) and various mixtures of PO enantiomers using chiral salen catalysts. The microstructures of the obtained copolymers as a function of polymerization time have been analyzed by a combination of chiral GC and high-resolution NMR spectroscopy. The ^{13}C NMR spectra of selected poly(propylene carbonate) samples were recorded using a 900 MHz (^1H) spectrometer, showing a previously unreported fine splitting of the carbonate resonances. This allowed a detailed assignment of signals for various copolymer microstructures taking into account the specifics in their stereo- and regioirregularities. For example, the enantioselectivity preference of the (*R*,*R*-salen)Co catalyst for (*S*)-PO at the beginning of the copolymerization leads predominantly to (*S*)-PO insertion, with any (*R*)-PO misinsertion being followed by incorporation of (*S*)-PO, so that the microstructure features isolated stereoerrors. K_{rel} calculations for the copolymerization showed around 5-fold enantioselectivity for (*S*)-PO over (*R*)-PO at short reaction time. Analysis of the copolymer microstructures obtained under various reaction conditions appears to be an additional approach to differentiate the occurrence of bimetallic and bifunctional copolymerization mechanisms that are widely discussed in the literature.

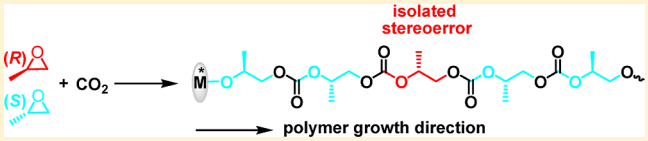

INTRODUCTION

Since the pioneering discovery of a catalytic system for the copolymerization of CO_2 and epoxides,[1−5] the utilization of CO_2 as a renewable C_1 feedstock has attracted great attention.[6−10] Specifically, the formation of alternating polycarbonates from a variety of epoxides is still a topic of current interest.[11−15] Understanding the ring-opening mode of propylene oxide (PO)[3] or styrene oxide (SO)[16,17] using the diethylzinc/water system was initially addressed by Inoue and co-workers, with the CO_2/(*R*)-PO copolymerization reaction showing a predominant (around 95%) ring-opening (RO) at the methylene position ("normal" RO).[3,18] By contrast, in the CO_2/(*R*)-SO copolymerization reaction, the methine group is predominantly attacked ("abnormal" RO), resulting in ∼96% inversion of stereoconfiguration (Scheme 1).[16−18]

Scheme 1. Differences of Epoxide Ring-Opening between Styrene Oxide and Propylene Oxide

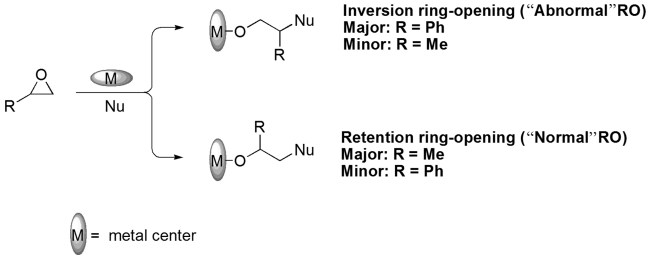

Early reports on the $^{13}C\{^1H\}$ NMR spectra of the CO_2/epoxide copolymers[16,17,19] have been followed by more detailed interpretation of the signals in the carbonate carbon region[20] with respect to the regiostructure of poly(propylene carbonate)s (PPC) (Figure 1). On the basis of both the aliphatic and carbonate carbon signals, Chisholm and co-workers investigated the regularity of alternating[21] and nonalternating PPC.[22]

The development of hydrolytic kinetic resolution (HKR) by Jacobsen and co-workers using chiral chromium[23] or cobalt[24,25] salen complexes to access the enantiomerically pure epoxides by ring-opening has inspired the investigation of chiral salen-type complexes for the synthesis of optically active polycarbonates.[26−34] Principally research has been devoted to the synthesis of new catalysts and study their chemical activity/selectivity as well as the mechanism and stereochemistry of the copolymerization reaction.[10] Consequently, new catalytic systems have been developed for propylene oxide,[32,35] styrene oxide,[36] epichlorohydrin,[37] and indene oxide[38] copolymerizations with CO_2. Specifically, cyclohexene oxide has been subjected to intense study with the realization that appropriate catalysts afford enantiomerically pure crystalline PCHC.[31,39,40] In addition, studies of CO_2/epoxide copolymer microstructures have attracted much attention. Stereoblock and stereogradient PPCs have been reported from CO_2/PO copolymerization

Received: September 12, 2012
Revised: October 18, 2012
Published: October 31, 2012

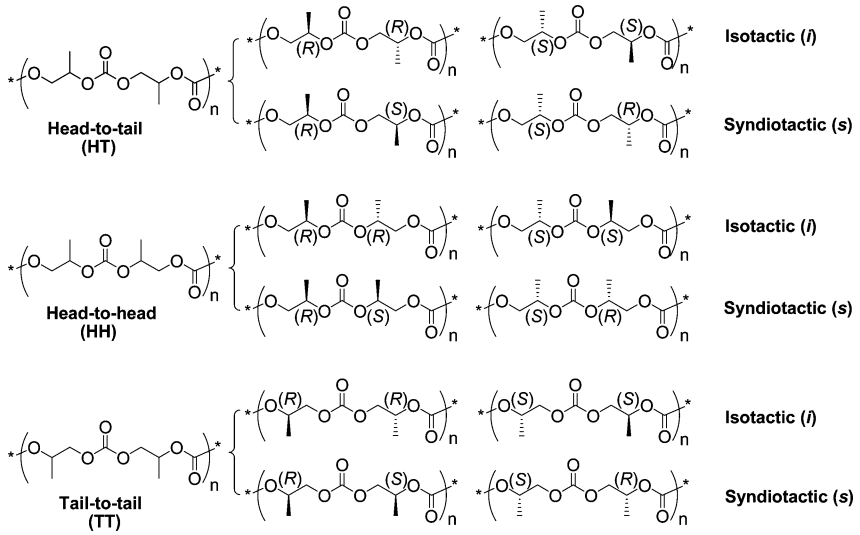

Figure 1. Regio- and stereochemistry around the carbonate carbons of PPC.

reactions, which showed different thermal stabilities.[35] Poly(styrene carbonate) (PSC)[41] has also been thoroughly studied, showing major "abnormal" ring-opening with predominant stereocenter inversion upon copolymerization of SO/CO_2 and is consistent with Inoue's earlier study.[16] Here we report an exploration of PPC microstructure using a combination of GC and high-resolution NMR spectroscopy. Our study concerns the regio- and stereostructure of PPC associated with the enantioselectivity of epoxide ring-opening during the copolymerization reaction as a function of reaction time and of increase in the number average molecular weight of the copolymer (M_n). The effect of cocatalyst and the nature of the catalytically active metal (Figure 2) on these parameters is

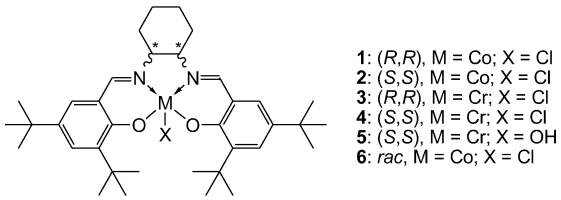

Figure 2. Structures of the applied salen complexes (**1**−**6**).

described. On the basis of the obtained results, we propose a more accurate assignment of ^{13}C NMR signals in the carbonate region of PPC and demonstrate that the ^{13}C NMR spectroscopic analysis of the PPC microstructure sheds light on the mechanistic peculiarities of CO_2/PO copolymerization such as the question of bimetallic or bifunctional chain propagation.

EXPERIMENTAL SECTION

Methods and Chemicals. All manipulations involving air- and/or moisture-sensitive compounds were carried out using standard Schlenk/glovebox techniques under an argon atmosphere unless otherwise stated. Propylene oxide was purchased from Acros and distilled under an argon atmosphere over CaH_2 prior to use. $Co(OAc)_2$ (anhydrous) was purchased from ABCR and stored in an argon-filled glovebox. CO_2 of purity grade 4.5 was purchased from Westfalen AG and was applied in all experiments without additional purification. Dry solvents were obtained with an MBraun MB-SPS-800 solvent purification system. All other chemicals were purchased from Aldrich and used as received without further purification. The enantiomeric excess (*ee*) of cyclic propylene carbonate was determined by chiral gas chromatography (GC). Gas chromatograms were obtained on a Varian CP-3380 using a flame ionization detector, N_2 carrier gas, and an Astec CHIRALDEX A-TA capillary GC column (30 m × 0.25 mm). Reference experiments with cyclic propylene carbonate (*rac*-cPC) were first performed to determine retention times. ^1H and $^{13}C\{^1H\}$ NMR spectra were collected at ambient temperature using Bruker AV-III 300, AV-III 500, or AV-III 900 spectrometers. The spectra were referenced against an internal standard (TMS for ^1H NMR spectra and $CDCl_3$ for ^{13}C NMR spectra). Number-average molecular weights (M_n) and polydispersity indices (M_w/M_n) were determined against PS standards by gel-permeation chromatography (GPC) using a Varian PL-GPC-50 Plus chromatograph equipped with a deflection RI detector. Tetrahydrofuran at 1 mL/min flow rate was used as eluent at 35 °C. Differential scanning calorimetry (DSC) measurements were performed on a TA DSC Q2000 in a temperature range from −50 to 150 °C in three cycles with a heating rate of 10 °C/min. Thermogravimetric analysis (TGA) was performed under an N_2 atmosphere on a TA TGA Q5000 in a temperature range between 40 and 650 °C with heating rate of 10 °C/min. Salen ligands[42] and complexes (**1**, **2**),[27] (**3**, **4**),[23] and **5**[43] were synthesized according to relevant literature procedures.

Representative CO_2/PO Copolymerization for Enantioselectivity Analysis. All polymerization experiments were performed in 100 mL steel autoclaves equipped with a magnetic stirring bar. The autoclave was prepared by heating at 130 °C overnight and cooling under vacuum to ambient temperature. The catalyst **1** (45.7 mg, 71.5 × 10^{-6} mol), bis(triphenylphosphine)iminium chloride ([PPN]Cl) (1.0, 0.5, or 0.25 molar ratio with respect to the catalyst), and propylene oxide (5.0 mL, 71.5 mmol, 1000 equiv with respect to catalyst) were transferred to the autoclave under an argon atmosphere. The autoclave was closed and then heated to 30 °C in an oil bath with stirring, followed by pressurization to 30 bar with CO_2. After the allotted reaction time, the autoclave was cooled to 0 °C and the pressure slowly released. An aliquot of the crude copolymer was taken for NMR spectroscopic analysis. The crude polymer was then dissolved in a minimal volume of dichloromethane and precipitated with methanolic HCl solution (2.2 M, 100 mL). This process was repeated three times to completely remove the catalyst, and the obtained colorless polymer was dried at 60 °C under vacuum to constant weight. The isolated PPC was weighed to calculate the yield and analyzed by ^1H and $^{13}C\{^1H\}$ NMR spectroscopy.

Degradation of PPC for GC Analysis. Degradation of the PPC was performed as previously published[21] with a slight modification. A Schlenk flask was charged with PPC (0.5 g) and purged with argon. Dry THF (25 mL) was then added, followed by LiO*t*Bu solution in

dx.doi.org/10.1021/ma301916r | *Macromolecules* 2012, 45, 8604−8613

Table 1. Copolymerization of CO_2/*rac*-PO Using Complex 1 and [PPN]Cl as Cocatalyst and 1000 equiv of PO with Respect to Complex 1 at 30 °C and 30 bar of CO_2

entry	cocat./cat. (equiv)	time (min)	selectivity (% PPC)[a]	yield (% PPC)[b]	carbonate linkages (%)[a]	M_n (kg/mol)[c]	PDI (M_w/M_n)[c]
1	1	30	64	12	≥98	14	1.3
2	1	60	90	27	≥99	16	1.4
3	1	90	96	40	≥99	22	1.4
4	1	120	98	51	≥99	29	1.2
5	1	180	99	53	≥98	29	1.5
6	1	240	99	65	≥99	28	1.5
7	0.5	30	88	9	≥99	10	1.2
8	0.5	60	96	15	≥99	18	1.2
9	0.5	90	97	21	≥99	19	1.2
10	0.5	120	97	28	≥99	27	1.3
11	0.5	180	98	41	≥99	33	1.2
12	0.5	240	98	50	≥99	38	1.2
13	0.5	360	99	65	≥99	45	1.2
14	0.25	60	98	15	≥99	14	1.2
15	0.25	120	98	20	≥99	22	1.3
16	0.25	180	99	32	≥99	26	1.4
17	0.25	240	99	49	≥99	30	1.5

[a]Determined by ^{1}H NMR spectroscopy (500 MHz). [b]Based on isolated PPC. [c]Determined by GPC in THF solution, against polystyrene standard.

THF (0.3 mL, 2.2 M, 0.66 mmol) and dry *tert*-butanol (1.0 mL) under an argon atmosphere. The reaction mixture was allowed to stir at 40 °C in a closed system. An NMR sample was then taken after 24 h to ensure the complete degradation of the polymer to cyclic propylene carbonate (cPC) (Supporting Information, Figures S1 and S2). All volatiles were then removed under reduced pressure, and the residue was dissolved in anhydrous chloroform (10 mL). For GC analysis 1 mL of this solution was diluted in chloroform (10 mL) and filtered using a 0.20 μm syringe filter prior to injection. ^{1}H NMR of cPC ($CDCl_3$, 300 MHz): δ 1.50 (d, 3H, CH_3), 4.03 (t, 1H, CH_2), 4.56 (t, 1H, CH_2), 4.86 (m, 1H, CH).

RESULTS AND DISCUSSION

According to literature data,[26,34] the activity of cobalt salen complexes toward CO_2/epoxide copolymerization can be increased by using binary catalyst systems. Consequently, the [(*t*-Bu)$_2$SalcyCo$^{(III)}$Cl] (**1**) together with [PPN]Cl was initially chosen for our studies (Table 1).

Variation of cocatalyst loading was shown to have a significant impact on PPC selectivity in the beginning of the copolymerization reaction. This effect was most pronounced when equimolar quantities of [PPN]Cl cocatalyst with respect to **1** were employed (Table 1, entry 1). In all cases, the PPC selectivity was observed to be independent of cocatalyst loading at longer reaction times with highly alternating polycarbonate structures obtained in all cases.

Polymer Microstructure. It is known that the PO ring-opening usually occurs at the epoxide methylene position via an S_N2 type mechanism ("normal" RO),[18] leading to a predominant head-to-tail (HT) regiostructure of the CO_2/PO copolymer. By contrast, tail-to-tail (TT) or head-to-head (HH) connectivities arise from the less favored PO ring-opening at the methine carbon ("abnormal" RO).

If enantiomerically pure (*R*)-PO is copolymerized with CO_2 using catalyst **1** (Table 2, entry 1), the resulting copolymer exhibits 88% HT connectivity with the remaining 12% equally distributed between HH and TT contributions (ca. 6% each), as was found by ^{13}C{^{1}H} NMR spectral analysis of the carbonate region (Figure 3a). After the degradation of this copolymer, 5% (*S*)-cPC and 95% (*R*)-cPC were detected by GC measurement, which shows that 95% of PO was incorporated into the copolymer with retention of configuration. The value of 5% for cPC with inverted configuration compares well with the amount of HH or TT junctions as was found by NMR spectroscopic analysis. This observation can be reasonably explained by an isolated regioerror model of the copolymer microstructure, according to which the less favored "abnormal" PO ring-opening at the methine carbon (associated with inversion of configuration) is immediately followed by ring-opening at the methylene center. The assignment of carbonate carbon signals at δ_C 153.8 and 154.8 ppm to HH and TT syndiotactic diads, respectively (Figure 4), is consistent with the previous work of Chisholm and co-workers.[44]

Table 2. Copolymerization of CO_2/PO Using [PPN]Cl as Cocatalyst and 1000 equiv of PO with Respect to Catalyst at 30 °C and 30 bar of CO_2 for 20 h

entry	cat.	PO	cocat./cat. (equiv)	carbonate linkage (%)[a]	HT (%)[b]	enantiopurity (%)[c]
1	**1**	*R*-	1	≥99	88	95.0 (*R*)
2	**2**	*R*-	1	≥99	94	99.0 (*R*)
3	**1**	*S*-	1	≥99	96	n.d.
4	**2**	*S*-	1	≥99	87	n.d.

[a]Determined by ^{1}H NMR spectroscopy (500 MHz). [b]Determined by ^{13}C{^{1}H} NMR spectroscopy (125 MHz). [c]Determined by GC. n.d.: not determined.

Copolymerization of enantiomerically pure (*R*)-PO with **2** (Table 2, entry 2) showed a lower degree of regioerrors in the ^{13}C{^{1}H} NMR spectrum of the copolymer (Figure 3b). The ^{13}C{^{1}H} NMR spectrum of this copolymer shows 94% HT content with both HH and TT contribution of around 3%. The HH region is represented by two peaks at δ_C 153.8 and 153.9 ppm. In the TT region, a shoulder of the peak at δ_C 154.8 ppm appears at the low-field side. GC analysis of the degraded copolymer showed 99% (*R*)-cPC (Table 2, entry 2) with 1% inversion, which indicates that ring-opening at the methine position (resulting in a regioerrors) occurred with both inversion and retention of the stereocenter configuration. Consequently, the additional HH and TT peaks are assigned as an isotactic diad structure (*i*) (Figure 3b,d).[44] Comparison of

dx.doi.org/10.1021/ma301916r | *Macromolecules* 2012, 45, 8604−8613

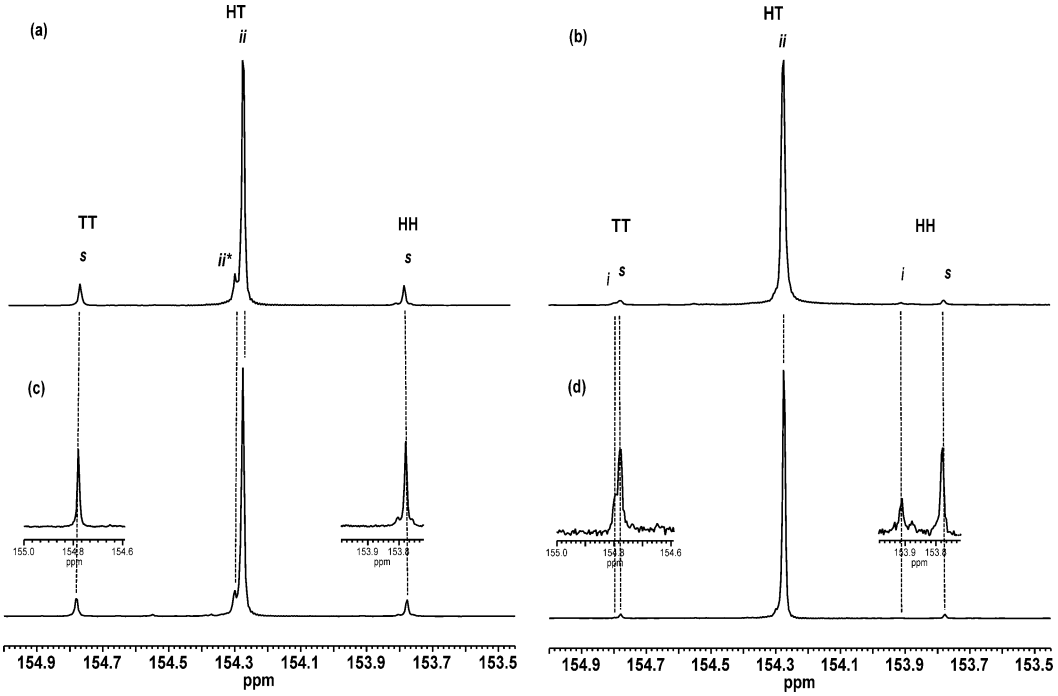

Figure 3. $^{13}C\{^{1}H\}$ NMR spectra (125 MHz, $CDCl_3$) of the carbonate carbon region for (a) (*R*)-PPC copolymer synthesized using **1**, (b) (*R*)-PPC copolymer synthesized using **2**, (c) (*S*)-PPC copolymer synthesized using **2**, (d) (*S*)-PPC copolymer synthesized using **1**, with 1 equiv of [PPN]Cl and 1000 equiv of PO at 30 °C and 30 bar of CO_2 for 20 h.

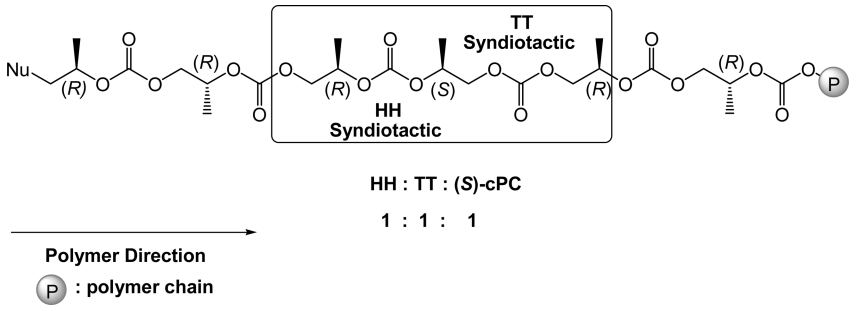

Figure 4. Syndiotactic HH and TT in (*R*)-PPC synthesized using **1**, resulting from "abnormal" epoxide ring-opening at the methine position.

the $^{13}C\{^{1}H\}$ NMR spectra (Figure 3) reveals that the signal of the PPC HT backbone prepared from (*R*)-PO or (*S*)-PO appears at the same chemical shift (δ_C 154.28 ppm), which is typical for a strictly alternating regioregular isotactic structure.[21,34] Remarkably, in the HT region of (*R*)-PPC prepared with catalyst **1** (Figure 3a), there is a small but clearly expressed downfield-shifted peak at δ_C 154.3 ppm, the intensity of which seems to be related to the intensity of the HH (or TT) signal. That is, in the case of (*S*)-PPC prepared with catalyst **1**, the intensity of the HH (or TT) signal is much lower and the minor peak in the HT region appears only as a small shoulder (Figure 3d). Although absolute integration of this shoulder resonance could not be reliably achieved, its intensity is approximately equal to that of the TT signal, allowing its assignment to the isotactic sequence adjacent to the regioerror, namely either *ii** or **ii* (the asterisk refers to a regioerror). Addition of 25% (*R*)-PO to (*S*)-PO and copolymerization for 1 h with CO_2 using catalyst **1** or **2** results in two significantly different copolymer microstructures. In the case of catalyst **1**, an *iso*-enriched copolymer with a low degree of regioerror is formed. Indeed, the peak corresponding to an isotactic sequence at δ_C 154.28 ppm is noticeably higher than all other signals. In addition, three low-intensity signals in the HT region are observed at δ_C 154.32, 154.34, and 154.39 ppm. Their intensity becomes comparable to that of the isotactic sequence peak if the catalyst **2** is applied (Figure 5).

Moreover, the conversion of the copolymer prepared with catalyst **2** is noticeably lower, which is a consequence of the reduced copolymerization rate. Simultaneously, this reduced degree of conversion results in a higher ratio of regioerror (Table 3) and is therefore associated with the selectivity of the chiral catalyst. Thus, the rate of (*S*)-PO copolymerization with (*R*,*R*)-configuration catalyst **1** is fast, whereas the (*S*,*S*)-configured catalyst **2** prefers (*R*)-PO and produces more regioerrors with the opposite (*S*)-PO enantiomer. The resonances observed in the carbonate carbon region of the $^{13}C\{^{1}H\}$ NMR spectra are best explained in terms of a model based on triad stereosequences,[34] taking into account the direction of the copolymer chain. That is, four signals of triads ($2^{(n-1)} = 2^2 = 4$),[45] namely *ii*, *is*, *si*, and *ss*, are expected, whereas the direction of the polymer chain causes the nonequivalence of the chemical shift for the *is* and *si* triads. The choice of chain direction is arbitrary, although it is preferable to associate this with the direction of copolymer chain growth (Figure 6). As

dx.doi.org/10.1021/ma301916r | *Macromolecules* 2012, 45, 8604−8613

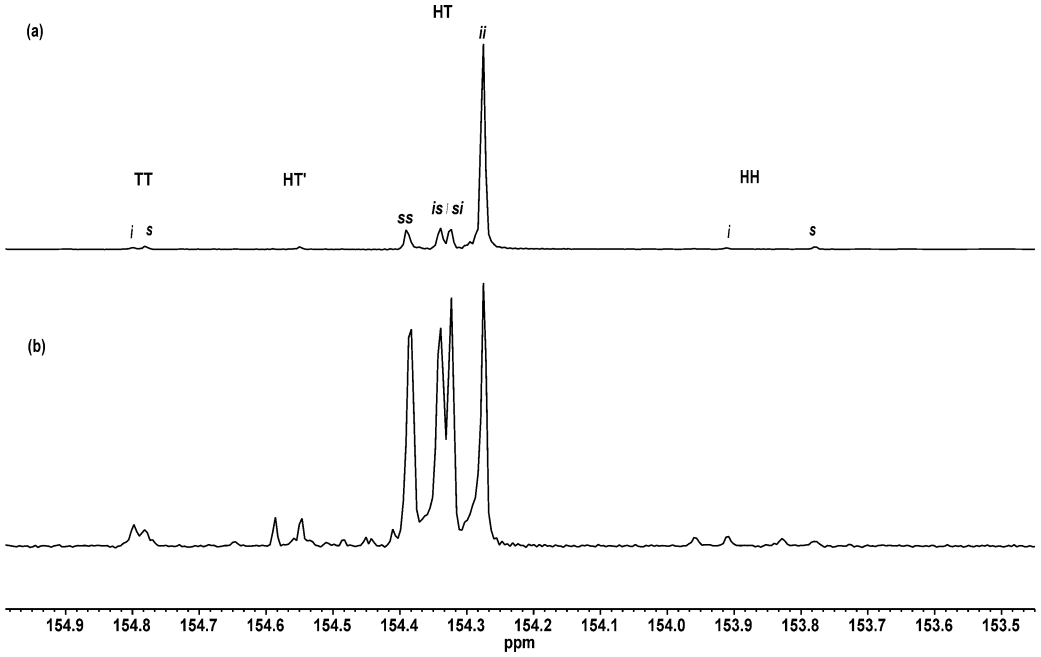

Figure 5. $^{13}C\{^{1}H\}$ NMR spectra (125 MHz, $CDCl_3$) of the carbonate carbon region for PPC copolymers synthesized with 1 equiv of [PPN]Cl, (a) using 75% (*S*)-PO and 25% (*R*)-PO and catalyst **1** and (b) using 75% (*S*)-PO and 25% (*R*)-PO and catalyst **2** (Table 3).

Table 3. Different Copolymerization Reactions of CO_2 Using 1000 equiv of PO and 1 equiv of [PPN]Cl with Respect to the Catalyst at 30 °C and 30 bar of CO_2

entry	cat.	PO (*S*)-PO:(*R*)-PO	time (h)	selectivity (% PPC)[a]	conv (% PPC)[a]	carbonate linkages (%)[a]	HT (%)[b]
1	**1**	75:25	1	93	40	≥99	96
2	**2**	75:25	1	65	9	≥97	93

[a]Determined by ^{1}H NMR spectroscopy (300 MHz). [b]Determined by $^{13}C\{^{1}H\}$ NMR spectroscopy (125 MHz).

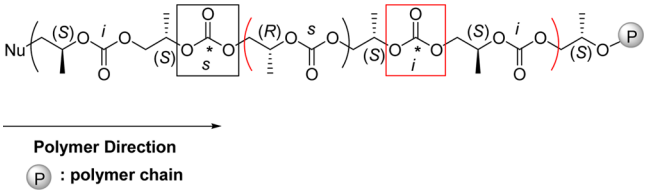

Figure 6. Effect of copolymer chain direction on *is* and *si* triads.

each triad structure contains three carbonate carbon atoms, the central carbon is assigned as the atom that gives rise to the signal of this particular triad (marked with an asterisk).

The asymmetry of the *is* and *si* triads is apparent from Figure 6. For the first triad, the corresponding carbonate carbon is surrounded by two stereocenters with opposite configurations (*R* and *S*), whereas for the second triad, the corresponding carbonate carbon is surrounded by stereocenters with the same configuration (*S* and *S*). At the beginning of the copolymerization reaction with *rac*-PO and catalyst **1**, (*S*)-PO is mostly incorporated into the copolymer with minimal insertion of (*R*)-PO. This leads to an *iso*-enriched copolymer with isolated stereoerrors, in which the intensities of *is*, *si*, and *ss* sequences should be equal. A similar spectral pattern was also found in the experiment with 75% (*S*)-PO:25% (*R*)-PO ratio using catalyst **1** (Figure 5a). In addition, CO_2/*rac*-PO copolymerization reactions were performed for different reaction times. The regio- and enantioselectivities have been estimated for the isolated copolymers using NMR spectroscopy and chiral GC (Table 4). Based on the triad structure inferred from the

Table 4. Microstructure Analysis Data for Copolymers from CO_2/*rac*-PO Using 1000 equiv of PO with Respect to the Catalyst 1 at 30 °C and 30 bar of CO_2

entry	cocat./cat. (equiv)	time (min)	TOF (h^{-1})[a]	HT (%)[b]	enantioselectivity (%)[c]	K_{rel}[d]
1	1	30	242	96	81.4 (*S*)	4.8
2	1	60	268	95	75.9 (*S*)	3.8
3	1	90	270	95	70.6 (*S*)	3.1
4	1	120	256	93	65.9 (*S*)	2.6
5	1	180	177	93	66.0 (*S*)	2.7
6	1	240	163	92	64.5 (*S*)	3.0
7	0.5	30	178	98	81.0 (*S*)	4.6
8	0.5	60	149	96	80.1 (*S*)	4.5
9	0.5	90	141	95	77.4 (*S*)	4.0
10	0.5	120	141	96	75.0 (*S*)	3.6
11	0.5	180	138	95	71.1 (*S*)	3.3
12	0.5	240	125	93	66.3 (*S*)	2.7
13	0.5	360	108	93	65.7 (*S*)	3.2
14	0.25	60	147	95	81.5 (*S*)	4.9
15	0.25	120	162	95	79.6 (*S*)	4.5
16	0.25	180	162	93	77.5 (*S*)	4.3
17	0.25	240	121	93	73.8 (*S*)	4.3

[a]Moles of the PPC/mol catalyst per time (h). [b]Determined by $^{13}C\{^{1}H\}$ NMR spectroscopy (125 MHz). [c]Determined by GC. [d]$K_{rel} = \ln[1 - c(1 + ee)]/\ln[1 - c(1 - ee)]$; c = conversion, ee = enantiomeric excess in the polymer.

$^{13}C\{^{1}H\}$ NMR spectra (HT carbonate carbon region), an average microstructure for the copolymer chains at different

dx.doi.org/10.1021/ma301916r | *Macromolecules* 2012, 45, 8604−8613

Table 5. Different Copolymerization Reactions of CO_2/*rac*-PO Using 1000 equiv of PO with Respect to the Catalyst at 30 °C and 30 bar of CO_2 for 2 h, without Cocatalyst

entry	cat.	conv (%)[a]	selectivity (PPC %)[a]	carbonate linkages (%)[a]	HT (%)[b]	M_n (kg/mol)[c]	PDI (M_w/M_n)[c]
1	**1**	22	100	≥97	82	19.7	1.2
2	**6**[d]	27	97	≥98	83	17.7	1.3

[a]Determined by ^{1}H NMR spectroscopy (500 MHz). [b]Determined by $^{13}C\{^1H\}$ NMR spectroscopy (125 MHz). [c]Determined by GPC in THF solution, calibrated with polystyrene standard. [d]Prepared by equimolar mixing of catalysts **1** and **2**.

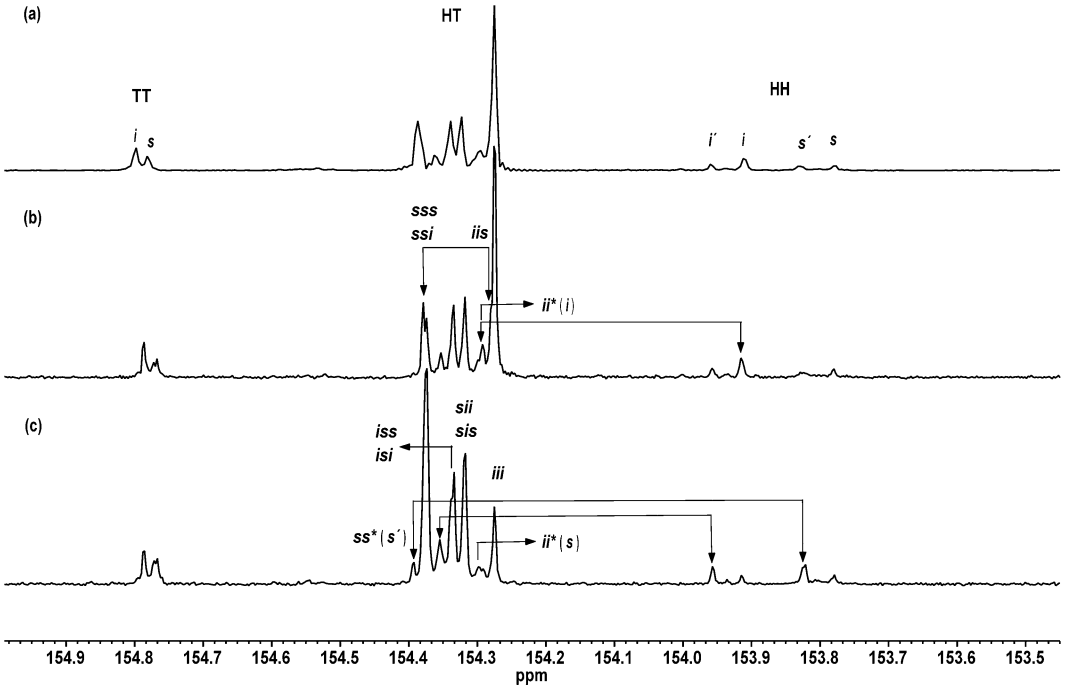

Figure 7. $^{13}C\{^1H\}$ NMR spectra of the carbonate carbon region of (a) *iso*-enriched PPC (125 MHz, $CDCl_3$) synthesized using **1**, (b) *iso*-enriched PPC (225 MHz, $CDCl_3$) synthesized using **1**, and (c) *syndio*-enriched PPC (225 MHz, $CDCl_3$) synthesized using **6** (Table 5) and the proposed assignment of signals on the tetrad level.

reactions time can be proposed based on NMR spectroscopic and GC analyses. The microstructure of the copolymers shows a gradient change of the copolymer sequences from *iso*-enriched to stereogradient microstructure due to the catalyst enantioselectivity. However, in-depth analysis of the spectral data reveals the presence of additional peaks at low intensity in the HT region. The relative intensity of these peaks increases with copolymerization time and is associated with the growth of signals in the TT and HH regions.

The appearance of minor peaks in the HT region of the $^{13}C\{^1H\}$ NMR spectra can be ascribed to the effect of regioerrors. The signal of the corresponding triad is shifted if it is located in the vicinity of the regioerror in the copolymer chain. Most probably, this effect is more pronounced when the regioerror is adjacent to the end of the stereosequence (see Figure 6), since in this case the spatial distance between the central carbon atom and the regioerror is smaller. If this is true, the integral intensity of the minor HT peaks should be equal to the intensity of the peaks in the TT or HH region. Additionally, from a statistical consideration the intensity of each minor signal should be proportional to the intensity of the corresponding parent triad signal. Unfortunately, the $^{13}C\{^1H\}$ NMR spectra recorded at 125 MHz are not sufficiently resolved for reliable integration. In this respect, higher frequency NMR spectroscopy was employed to obtain further information. Two different *iso*-enriched and *syndio*-enriched copolymers were synthesized (Table 5). Both samples were analyzed using high-resolution (both 125 and 225 MHz) NMR spectroscopy (Figure 7). The increase in frequency clearly results in a higher resolution of the signals in both the HT and TT regions.

For the *iso*-enriched copolymer (Figure 7b), the signal assigned as *ii* shows a downfield shoulder whereas the *ss* signal splits into two, which necessitates the consideration of the influence of the neighboring stereocenters and application of a tetrad model for the signals of various stereosequences (taking into account the direction of the copolymer according to the above-listed considerations). Interestingly, for the *syndio*-enriched copolymer, the splitting of the signal assigned to the *is*-triad (Figure 7c) was observed as a shoulder, whereas the highest signal of the *ss*-triad was resolved as a single peak. However, a new low-intensity peak in the vicinity of the *ss*-signal in the lower field region was observed that could be assigned to an effect of a regioerror close to the syndiotactic triad. Accordingly, all observed low-intensity signals (δ_C 154.29, 154.30, 154.35, and 154.39 ppm) correlate well with the resonances in the HH and TT regions due to the regioerror (Figure 7).

For comparison with the Co-based catalyst, the (*R*,*R*)-[(*t*-Bu)$_2$SalcyCr$^{(III)}$Cl]/DMAP (**3**) system was tested with two different (*S*)-PO:(*R*)-PO ratios (1:3 and 3:1, respectively) which showed the preference of this catalyst for (*S*)-PO. However, this Cr-based system leads to copolymers with a high

dx.doi.org/10.1021/ma301916r | *Macromolecules* 2012, 45, 8604−8613

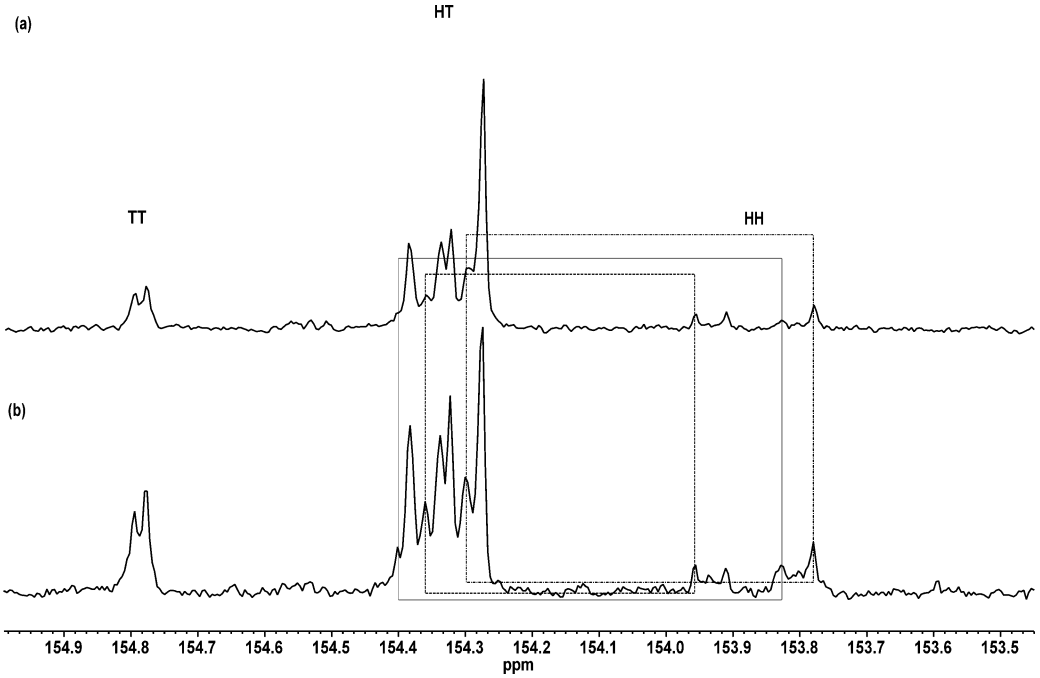

Figure 8. $^{13}C\{^{1}H\}$ NMR spectra (75 MHz, $CDCl_3$) of the carbonate carbon region for PPC copolymer synthesized using catalyst **3** with 0.5 equiv of DMAP, (a) using 75% (*S*)-PO and 25% (*R*)-PO and (b) using 25% (*S*)-PO and 75% (*R*)-PO at 50 °C and 50 bar of CO_2 for 20 h.

Table 6. Different Copolymerization Reactions of CO_2/(*R*)-PO Using 1400 equiv of PO with Respect to the Catalyst at Ambient Temperature and 50 bar of CO_2 for 48 h, without Cocatalyst

entry	cat.	yield (%)[a]	selectivity (% PPC)[b]	carbonate linkages (%)[b]	HT (%)[c]	M_n (kg/mol)[d]	PDI (M_w/M_n)[d]
1	**4**	5.2	≥99	≥92	79	8.0	1.4
2	**5**	5.5	≥99	≥89	80	7.0	1.4

[a]Based on isolated yield of the copolymer. [b]Determined by ^{1}H NMR spectroscopy (500 MHz). [c]Determined by $^{13}C\{^{1}H\}$ NMR spectroscopy (125 MHz). [d]Determined by GPC in THF solution, against polystyrene standard.

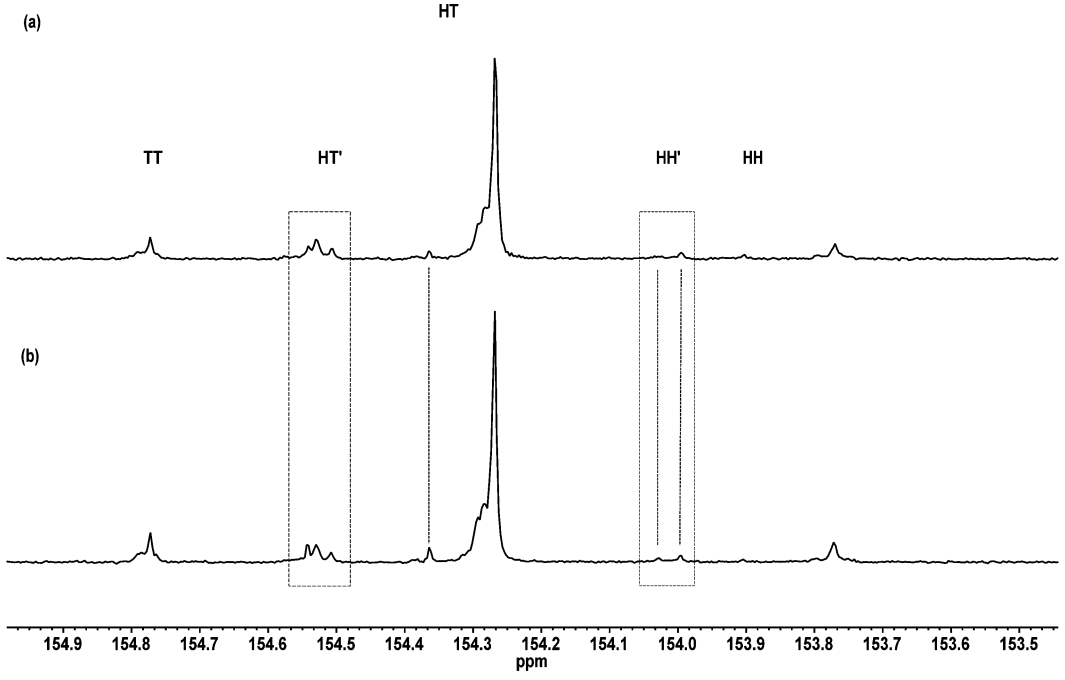

Figure 9. $^{13}C\{^{1}H\}$ NMR spectra (125 MHz) of the carbonate carbons region for PPC copolymer, (a) synthesized using **4** and (b) synthesized using **5**, with 1400 equiv (*R*)-PO and 50 bar of CO_2 without cocatalyst (Table 6).

dx.doi.org/10.1021/ma301916r | *Macromolecules* 2012, 45, 8604−8613

regioerror ratio compared to the Co-based catalyst as can be seen from the intensity of the signals in the HH and TT regions (Figure 8).

The higher intensity of the TT signal is accompanied by an associated higher intensity of the signals in the HT region which correlates with regioerrors (*ii*$_*$/$_*$*ii*, *si*$_*$/$_*$*is*, *is*$_*$/$_*$*is*, and *ss*$_*$/$_*$*ss*) and is consistent with the proposed assignment model. Aside from the HT region, the splitting pattern of the signals in the HH region of the spectrum is informative with respect to the copolymer microstructure. The splitting of the signals in the TT region is not pronounced, therefore indicating a weak influence of the neighboring stereoconfiguration on the chemical shift of this junction. It is therefore expected that the HH junction has a stronger affect on the chemical shifts neighboring stereosequences than the TT sequence. This has been verified from the ratio of HH:TT:*ii*$_*$ peak areas of the (*R*)-PPC (Figure 3a), since this was found to be approximately 1:1:1 and not 1:1:2. The assignment of HH signals to *i* or *s* diads has already been reported and was verified in our study using GC measurements. On the basis of this, we have proposed the assignment of four peaks in this region as shown in Figure 7. Importantly, a greater number of peaks in the HH region can be observed for copolymers with a high degree of regioerrors, for which the model of isolated regioerror is no longer valid. The origin of *i*-diads in the HH region is referred to an "abnormal" PO-enchainment with retention of configuration of the stereocenters. This would imply either an S_N1-type ring-opening mechanism or an S_N2-type with retention of configuration, both unusual for propylene oxide.[18] Chisholm and co-workers have reported that the (*R*,*R*-salen)Cr catalyst (**3**) prefers the "abnormal" ring-opening of (*S*)-PO in copolymerization with CO_2 to generate the primary alkoxide with (*S*)-configuration,[44] with which a high intensity of the *i*-diad signal in the HH region compared to the *s*-diad is observed. In order to verify whether this phenomenon could be connected with the nature of the initiating group of the catalyst, copolymers produced from (*R*)-PO/CO_2 copolymerization by two (*S*,*S*-salen)CrX catalysts, namely **4** (X = Cl) and **5** (X = OH), were compared (Table 6).

Although these reactions represent a "mirror stereochemistry" of Chisholm's system discussed above with respect to the catalyst and propylene oxide configuration, it is surprising that nearly no "abnormal" ring-opening of PO with retention of configuration in the present system was observed. Both catalysts **4** and **5** produced very similar copolymers in terms of molecular weight and microstructure (Figure 9). However, the copolymers feature an increased content of ether linkages compared with the previously described systems that is reflected in new peaks in the HT region. A group of peaks appeared at δ_C 154.5−154.6 ppm, and a new shoulder of the *ii* signal is clearly seen at the low-field side in addition to the *ii*$_*$ resonance. Unfortunately, the high amount of both regioerror and PO misinsertion (alternation error) prohibits the unambiguous assignment of each signal in these copolymers using the isolated error approach.

Copolymerization Mechanism. From the above, a mechanism of the catalyst stereoselectivity in copolymerization can be proposed. Since the (*R*,*R*)-catalyst prefers (*S*)-PO insertion, it is clear that *iso*-enriched copolymer forms at the beginning of the reaction. At this stage, any (*R*)-PO insertion leads predominantly to "normal" ring-opening to form the HT regiostructure with a syndiotactic stereosequence. This misinsertion is then "corrected" by a (*S*)-PO insertion, thus producing an isotactic sequence with isolated stereoerrors. With gradual consumption of (*S*)-PO and increase of (*R*)-PO in the reaction feed, the relative insertion of the latter increases and the overall copolymer growth becomes slower. At high PO conversion, the "abnormal" ring-opening becomes more pronounced, therefore increasing the HH and TT ratios in the copolymer. At this point, the copolymer can be described as an *iso*-enriched stereogradient copolymer. GC measurements of the degraded copolymers allowed the determination of K_{rel} according to the equation $K_{rel} = \ln[1 - c(1 + ee)]/\ln[1 - c(1 - ee)]$, where K_{rel} corresponds to the difference in energy between the diastereomeric transition states in the selectivity-determining step of the catalytic reaction.[46] The K_{rel} values (Table 4) showed that the insertion of (*S*)-PO is around 5 times more favored than (*R*)-PO at the beginning of the reaction. With consumption of (*S*)-PO, the K_{rel} values decrease correspondingly, which is a known issue.[46] Detailed $^{13}C\{^1H\}$ NMR spectroscopic analysis of the microstructure of the produced copolymers allowed us to distinguish between the two operating mechanisms of copolymerization. Our conclusions are based on the following facts: (i) copolymerization of *rac*-PO with CO_2 using the enantiomeric pure (*R*,*R*)-catalyst gives *iso*-enriched copolymer at the beginning of the reaction, (ii) the same system in the presence of [PPN]Cl as cocatalyst also affords *iso*-enriched polymer, and (iii) copolymerization of *rac*-PO with CO_2 using an equimolar mixture of (*R*,*R*)- and (*S*,*S*)-configuration catalysts leads to an almost atactic polymer in the presence of [PPN]Cl as cocatalyst (Figure S9), whereas (iv) in the absence of cocatalyst a *syndio*-enriched copolymer is formed (Figure 7c). All our observations strongly support a dynamic nature of copolymerization, namely that the growing polymer chain can easily dissociate from one metal center and coordinate to the another active site, especially in the presence of a cocatalyst due to the formation of an anionic hexacoordinated species. This is closely associated with the so-called binary mechanism, according to which PO is activated by coordination to a metal center, followed by an attack of a noncoordinated nucleophilic polymer chain end. In this case, there is no or little chain end control of the microstructure, since the chiral center of the chain is remote from the nucleophilic center of the chain (O atom of the carbonate group). Respectively, the ring-opening of coordinated (*R*)-PO at an (*S*,*S*)-catalyst or of (*S*)-PO at (*R*,*R*)-configuration by the noncoordinated chain end would proceed at an equal rate, leading to an almost atactic polymer (case iii). However, in the absence of cocatalyst, the dissociation of the polymer chain end from the metal center is slowed (anionic complexes are practically absent in the reaction media), and copolymerization occurs via a bimetallic mechanism, according to which the carbonate chain end coordinated at one metal center attacks an activated PO at another metal site. This reaction pathway is generally slower than the binary propagation but provides a good explanation for the formation of *syndio*-enriched polymer (case iv). Moreover, the syndiotacticity of the obtained copolymer indicates that the copolymerization reaction preferably occurs via interaction of two catalyst molecules with opposite stereoconfigurations (i.e., (*S*,*S*)- and (*R*,*R*)-configuration). Independently, both bimetallic and binary mechanisms would lead to *iso*-enriched polymers if only one stereoisomer of the catalyst ((*R*,*R*) or (*S*,*S*)) is employed in the copolymerization of *rac*-PO and CO_2, which is largely due to the stereoselectivity in PO coordination. These conclusions are consistent with various previous reports on the copolymeriza-

dx.doi.org/10.1021/ma301916r | *Macromolecules* 2012, 45, 8604−8613

tion mechanism of PO and CO_2, which were based on studies of the reaction kinetics and other investigations.[43,47]

Thermal Properties of the PPC Copolymers. DSC and TGA analyses have been applied for all the copolymers listed in Tables 1 and 4, which have been compared to those of the enantiomeric pure (*R*)-PPC (Figures S10 and S11). Table 7

Table 7. DSC and TGA Measurements for the Different Copolymers Obtained in Table 4

entry	T_g	T_{d5} [a]	T_{d50} [a]	T_{d95} [a]
1	37	229.7	253.3	295.9
2	38	225.6	243.2	278.2
3	38	222.5	243.1	272.0
4	39	223.1	247.2	277.2
5	38	203.2	224.4	258.0
6	38	219.8	239.1	276.2
7	35	240.1	253.9	287.8
8	37	229.9	247.2	278.4
9	38	225.8	243.2	267.0
10	37	233.3	252.0	280.1
11	39	220.3	233.3	264.4
12	38	221.2	230.6	256.6
13	40	202.1	229.4	268.9
14	34	215.1	231.7	263.3
15	39	227.1	244.4	275.4
16	39	217.4	239.9	274.4
17	40	212.4	235.1	267.3
18[b]	39	240.6	255.8	288.4

[a] T_{d5}, T_{d50}, and T_{d95} are the decomposition temperature at 5%, 50%, and 95% weight loss, respectively. For the synthetic conditions, see the corresponding entry in Tables 1 and 4. [b] (*R*)-PPC (Table 2, entry 2).

clearly shows that there is no correlation between the microstructure, M_n, and the physical properties of the produced *iso*-enriched stereogradient copolymers. DSC measurements in the range of −50 to 150 °C showed only a glass transition temperature (T_g) without any indication of crystallization. Even a highly stereo- and regioregular PPC (Table 7, entry 18) obtained in our work could not be crystallized.[48]

The thermal degradation pathway of PPC has been previously reported to occur by either a main chain random scission or by unzipping (backbiting) degradation.[49−51] Herein, the decomposition pathway and the decomposition products have been followed by TGA and TGA/MS. A representative copolymer with M_n of 24.2 kg/mol was divided into three samples and heated under N_2 to 150, 200, and 240 °C. Upon cooling, the solidified residues were analyzed by GPC with the resulting M_n determined to be 22.8 kg/mol (1% weight loss), 22.3 kg/mol (2% weight loss), and 12.3 kg/mol (30% weight loss), respectively. Additionally, the TGA/MS measurements showed that the mass spectra of the copolymer degradation products are identical to the mass spectrum of cPC. Consequently, it is proposed that the thermal degradation of the obtained copolymers occurs mainly through an unzipping (backbiting) mechanism rather than a random main chain scission. It is believed that an influence of the microstructure of the studied copolymers on the TGA data could not be observed because various other parameters have a significant impact onto the thermal stability of the PPC, which cannot be easily controlled. Among these are residual impurities (solvents, metal residues, acids, cPC byproduct), polyether inclusion, end groups, additives, molecular weight, and purity of the PPC.[52−61]

CONCLUSION

The selectivity of the chiral catalyst **1** for (*S*)-PO over (*R*)-PO during the *rac*-PO/CO_2 copolymerization reaction led to the synthesis of stereogradient PPCs with different (*S*)-PO ratios in the copolymer chain. As incorporation of (*S*)-PO in the polymer chain is 5 times faster than (*R*)-PO, the copolymerization reaction becomes slower with an increase of (*R*)-PO concentration in the reaction feed, therefore indicating that (*S*)-PO insertion has a crucial influence on the microstructure. A change of cocatalyst loading did not show any effect on the PPC microstructure. Following of the (*S*)-PO/(*R*)-PO ratios in the polymer chain during the *rac*-PO/CO_2 copolymerization reaction using GC and 500 MHz NMR spectroscopy led to the understanding of PPC microstructure during copolymer growth and aided the assignment of the carbonate carbon signal in the associated $^{13}C\{^1H\}$ NMR spectra taking into consideration the direction of the copolymer chain. DSC measurements did not show any correlation between the glass transition temperature of the stereogradient copolymers and the microstructure; however, TGA/MS measurements showed that main thermal decomposition pathway of PPC is a chain unzipping pathway, resulting in cPC.

ASSOCIATED CONTENT

Supporting Information

^1H NMR spectra of the copolymer degradation products; GC chromatogram for *rac*-cyclic propylene carbonate and representative (*S*)-enriched cyclic propylene carbonate; DSC and TGA curves; $^{13}C\{^1H\}$ NMR spectrum of almost atactic PPC. This material is available free of charge via the Internet at http://pubs.acs.org.

AUTHOR INFORMATION

Corresponding Author

*E-mail: rieger@tum.de.

Notes

The authors declare no competing financial interest.

ACKNOWLEDGMENTS

This publication is based on work supported by Award KSAC0069/UK-C0020, made by the King Abdullah University of Science and Technology (KAUST).

REFERENCES

(1) Inoue, S.; Koinuma, H.; Tsuruta, T. *Makromol. Chem.* **1969**, *130*, 210−220.
(2) Inoue, S.; Koinuma, H.; Tsuruta, T. *J. Polym. Sci., Part B* **1969**, *7*, 287−292.
(3) Inoue, S.; Koinuma, H.; Tsuruta, T. *Polym. J.* **1971**, *2*, 220−224.
(4) Kobayashi, M.; Inoue, S.; Tsuruta, T. *Macromolecules* **1971**, *4*, 658−659.
(5) Inoue, S.; Koinuma, H.; Yokoo, Y.; Tsuruta, T. *Makromol. Chem.* **1971**, *143*, 97−104.
(6) Decortes, A.; Castilla, A. M.; Kleij, A. W. *Angew. Chem., Int. Ed.* **2010**, *49*, 9822−9837.
(7) Cokoja, M.; Bruckmeier, C.; Rieger, B.; Herrmann, W. A.; Kuehn, F. E. *Angew. Chem., Int. Ed.* **2011**, *50*, 8510−8537.
(8) Martin, R.; Kleij, A. W. *ChemSusChem* **2011**, *4*, 1259−1263.
(9) Peters, M.; Koehler, B.; Kuckshinrichs, W.; Leitner, W.; Markewitz, P.; Mueller, T. E. *ChemSusChem* **2011**, *4*, 1216−1240.
(10) Quadrelli, E. A.; Centi, G.; Duplan, J.-L.; Perathoner, S. *ChemSusChem* **2011**, *4*, 1194−1215.
(11) Darensbourg, D. J. *Inorg. Chem.* **2010**, *49*, 10765−10780.

(12) Brule, E.; Guo, J.; Coates, G. W.; Thomas, C. M. *Macromol. Rapid Commun.* **2011**, *32*, 169−185.
(13) Kember, M. R.; Buchard, A.; Williams, C. K. *Chem. Commun.* **2011**, *47*, 141−163.
(14) Klaus, S.; Lehenmeier, M. W.; Anderson, C. E.; Rieger, B. *Coord. Chem. Rev.* **2011**, *255*, 1460−1479.
(15) Lu, X.-B.; Darensbourg, D. J. *Chem. Soc. Rev.* **2012**, *41*, 1462−1484.
(16) Hirano, T.; Inoue, S.; Tsuruta, T. *Makromol. Chem.* **1975**, *176*, 1913−1917.
(17) Inoue, S.; Hirano, T.; Tsuruta, T. *Polym. J.* **1977**, *9*, 101−106.
(18) Parker, R. E.; Isaacs, N. S. *Chem. Rev.* **1959**, *59*, 737−799.
(19) Rokicki, A.; Kuran, W. *Makromol. Chem.* **1979**, *180*, 2153−2161.
(20) Lednor, P. W.; Rol, N. C. *J. Chem. Soc., Chem. Commun.* **1985**, 598−599.
(21) Chisholm, M. H.; Navarro-Llobet, D.; Zhou, Z. *Macromolecules* **2002**, *35*, 6494−6504.
(22) Byrnes, M. J.; Chisholm, M. H.; Hadad, C. M.; Zhou, Z. *Macromolecules* **2004**, *37*, 4139−4145.
(23) Martinez, L. E.; Leighton, J. L.; Carsten, D. H.; Jacobsen, E. N. *J. Am. Chem. Soc.* **1995**, *117*, 5897−5898.
(24) Tokunaga, M.; Larrow, J. F.; Kakiuchi, F.; Jacobsen, E. N. *Science* **1997**, *277*, 936−938.
(25) Schaus, S. E.; Brandes, B. D.; Larrow, J. F.; Tokunaga, M.; Hansen, K. B.; Gould, A. E.; Furrow, M. E.; Jacobsen, E. N. *J. Am. Chem. Soc.* **2002**, *124*, 1307−1315.
(26) Lu, X.-B.; Wang, Y. *Angew. Chem., Int. Ed.* **2004**, *43*, 3574−3577.
(27) Lu, X.-B.; Shi, L.; Wang, Y.-M.; Zhang, R.; Zhang, Y.-J.; Peng, X.-J.; Zhang, Z.-C.; Li, B. *J. Am. Chem. Soc.* **2006**, *128*, 1664−1674.
(28) Li, B.; Wu, G.-P.; Ren, W.-M.; Wang, Y.-M.; Rao, D.-Y.; Lu, X.-B. *J. Polym. Sci., Part A: Polym. Chem.* **2008**, *46*, 6102−6113.
(29) Min, S. S. J. K.; Seong, J. E.; Na, S. J.; Lee, B. Y. *Angew. Chem., Int. Ed.* **2008**, *47*, 7306−7309.
(30) Nakano, K.; Hashimoto, S.; Nozaki, K. *Chem. Sci.* **2010**, *1*, 369−373.
(31) Ren, W.-M.; Zhang, X.; Liu, Y.; Li, J.-F.; Wang, H.; Lu, X.-B. *Macromolecules* **2010**, *43*, 1396−1402.
(32) Ren, W.-M.; Liu, Y.; Wu, G.-P.; Liu, J.; Lu, X.-B. *J. Polym. Sci., Part A: Polym. Chem.* **2011**, *49*, 4894−4901.
(33) Qin, Z.; Thomas, C. M.; Lee, S.; Coates, G. W. *Angew. Chem., Int. Ed.* **2003**, *42*, 5484−5487.
(34) Cohen, C. T.; Chu, T.; Coates, G. W. *J. Am. Chem. Soc.* **2005**, *127*, 10869−10878.
(35) Nakano, K.; Hashimoto, S.; Nakamura, M.; Kamada, T.; Nozaki, K. *Angew. Chem., Int. Ed.* **2011**, *50*, 4868−4871.
(36) Wu, G.-P.; Wei, S.-H.; Lu, X.-B.; Ren, W.-M.; Darensbourg, D. J. *Macromolecules* **2010**, *43*, 9202−9204.
(37) Wu, G.-P.; Wei, S.-H.; Ren, W.-M.; Lu, X.-B.; Xu, T.-Q.; Darensbourg, D. J. *J. Am. Chem. Soc.* **2011**, *133*, 15191−15199.
(38) Darensbourg, D. J.; Wilson, S. J. *J. Am. Chem. Soc.* **2011**, *133*, 18610−18613.
(39) Kember, M. R.; Jutz, F.; Buchard, A.; White, A. J. P.; Williams, C. K. *Chem. Sci.* **2012**, *3*, 1245−1255.
(40) Wu, G.-P.; Ren, W.-M.; Luo, Y.; Li, B.; Zhang, W.-Z.; Lu, X.-B. *J. Am. Chem. Soc.* **2012**, *134*, 5682−5688.
(41) Wu, G.-P.; Wei, S.-H.; Ren, W.-M.; Lu, X.-B.; Li, B.; Zu, Y.-P.; Darensbourg, D. J. *Energy Environ. Sci.* **2011**, *4*, 5084−5092.
(42) Larrow, J. F.; Jacobsen, E. N.; Gao, Y.; Hong, Y.; Nie, X.; Zepp, C. M. *J. Org. Chem.* **1994**, *59*, 1939−1942.
(43) Klaus, S.; Vagin, S. I.; Lehenmeier, M. W.; Deglmann, P.; Brym, A. K.; Rieger, B. *Macromolecules* **2011**, *44*, 9508−9516.
(44) Chisholm, M. H.; Zhou, Z. *J. Am. Chem. Soc.* **2004**, *126*, 11030−11039.
(45) Thakur, K. A. M.; Kean, R. T.; Hall, E. S.; Kolstad, J. J.; Lindgren, T. A.; Doscotch, M. A.; Siepmann, J. I.; Munson, E. J. *Macromolecules* **1997**, *30*, 2422−2428.
(46) Keith, J. M.; Larrow, J. F.; Jacobsen, E. N. *Adv. Synth. Catal.* **2001**, *343*, 5−26.
(47) Ren, W.-M.; Wu, G.-P.; Lin, F.; Jiang, J.-Y.; Liu, C.; Luo, Y.; Lu, X.-B. *Chem. Sci.* **2012**, *3*, 2094−2102.
(48) Luinstra, G. A. *Polym. Rev.* **2008**, *48*, 192−219.
(49) Liu, B.; Chen, L.; Zhang, M.; Yu, A. *Macromol. Rapid Commun.* **2002**, *23*, 881−884.
(50) Li, X. H.; Meng, Y. Z.; Zhu, Q.; Tjong, S. C. *Polym. Degrad. Stab.* **2003**, *81*, 157−165.
(51) Lu, X. L.; Zhu, Q.; Meng, Y. Z. *Polym. Degrad. Stab.* **2005**, *89*, 282−288.
(52) Dixon, D. D.; Ford, M. E.; Mantell, G. J. *J. Polym. Sci., Polym. Lett. Ed.* **1980**, *18*, 131−134.
(53) Kuran, W.; Listos, T. *Macromol. Chem. Phys.* **1994**, *195*, 1011−1015.
(54) Liu, B.; Zhao, X.; Wang, X.; Wang, F. *J. Appl. Polym. Sci.* **2003**, *90*, 947−953.
(55) Peng, S.; An, Y.; Chen, C.; Fei, B.; Zhuang, Y.; Dong, L. *Polym. Degrad. Stab.* **2003**, *80*, 141−147.
(56) Gao, L. J.; Du, F. G.; Xiao, M.; Wang, S. J.; Meng, Y. Z. *J. Appl. Polym. Sci.* **2008**, *108*, 3626−3631.
(57) Gao, L. J.; Xiao, M.; Wang, S. J.; Meng, Y. Z. *J. Appl. Polym. Sci.* **2008**, *108*, 1037−1043.
(58) Spencer, T. J.; Kohl, P. A. *Polym. Degrad. Stab.* **2011**, *96*, 686−702.
(59) Yao, M.; Mai, F.; Deng, H.; Ning, N.; Wang, K.; Fu, Q. *J. Appl. Polym. Sci.* **2011**, *120*, 3565−3573.
(60) Yu, T.; Luo, F.-L.; Zhao, Y.; Wang, D.-J.; Wang, F.-S. *J. Appl. Polym. Sci.* **2011**, *120*, 692−700.
(61) Barreto, C.; Hansen, E.; Fredriksen, S. *Polym. Degrad. Stab.* **2012**, *97*, 893−904.